

Odd triplet superconductivity in clean and moderately disordered SFFS junctions

Zorica Popović and Zoran Radović

Department of Physics, University of Belgrade, P.O. Box 368, 11001 Belgrade, Serbia

We study the Josephson effect and pairing correlations in SFFS junctions that consist of conventional superconductors (S) connected through two metallic monodomain ferromagnets (F) with transparent and spin inactive interfaces. We solve the Eilenberger equations for arbitrary relative orientation of magnetizations of the two F layers in the clean limit and for moderate disorder in ferromagnets. Spatial variation of pair amplitudes, singlet f_s , and odd in frequency triplet f_{t0} and f_{t1} , with 0 and ± 1 spin projections, as well as the Josephson current-phase relations are calculated for different values of the ferromagnetic layers thickness and angle α between in-plane magnetizations. In contrast to the dirty limit case, we find that for $0 < \alpha < \pi$ both spin singlet and triplet pair amplitudes in F layers power-law decay in the same oscillatory manner with distance from the FS interfaces. This decay gets faster as the impurity-scattering rate in ferromagnets is increased. The computed triplet amplitude f_{t1} has opposite signs in the two magnet regions, penetrates into the superconductors and monotonically decays over the same distance, which is the superconducting coherence length, as the singlet amplitude f_s saturates to the bulk value. We point out that influence of misorientation of magnetizations on the Josephson current can not be attributed directly to the appearance of odd triplet correlations.

PACS numbers: 74.45.+c, 74.50.+r

I. INTRODUCTION

Odd-frequency triplet superconducting correlations with non-zero total spin projection induced by proximity effect in heterostructures containing superconductors with ordinary singlet pairing and inhomogeneous ferromagnets have been of considerable interest in the last decade.^{1,2,3,4,5,6} Odd-frequency pairing mechanism was proposed long ago in an attempt to describe the A phase of superfluid ^3He .⁷ Although this superconducting state is thermodynamically stable,⁸ it was found that in the case of superfluid ^3He the pairing is odd in space (p -wave) rather than in time, "odd" triplet superconductivity occurs in certain superconductor-ferromagnet (SF) structures.⁴ It is believed that this exotic s -wave pairing state which is even in momentum, but with the triplet correlations being odd in frequency, can enhance significantly the superconducting penetration length at the SF interface,³ providing a Josephson current through half-metallic barriers.^{4,5,6} The simplest examples of SF heterostructures with inhomogeneous magnetization are FSF and SFFS heterojunctions with homogeneous monodomain ferromagnetic layers having an angle α between their in-plane magnetizations. These structures have been studied using quasiclassical approach in both diffusive^{1,2,3,9,10,11,12,13} and clean^{14,15,16} limits by solving Usadel¹⁷ and Eilenberger¹⁸ equations, respectively, and by solving the Bogoliubov-de Gennes equation.^{6,19,20,21,22} In the case of parallel ($\alpha = 0$) magnetizations, SFS junctions,^{23,24} besides spin-singlet superconducting correlations, only odd triplet correlations with zero total spin projection exist. These correlations penetrate into the ferromagnet over a short length scale determined by the exchange energy. For noncollinear magnetizations, triplet correlations with nonzero spin projection are present as well. It is expected that they are not sup-

pressed by the exchange interaction, and consequently that they are long ranged.² It has been predicted for diffusive junctions that long-range spin-triplet components with spin projection ± 1 should have a dramatic impact on transport properties and the Josephson effect, displayed through a nonmonotonic dependence on angle between magnetizations. In diffusive Josephson junctions, the length scales associated with short- and long-range correlations are, respectively, $\xi_F^d = \sqrt{\hbar D_F/h_0}$ and $\xi_N^d = \sqrt{\hbar D_F/k_B T}$, where D_F is the diffusion constant in the ferromagnet, and thermal energy $k_B T$ is typically much smaller than the exchange energy h_0 . However, this is not the case in ballistic SF heterostructures in which the only characteristic length is the ferromagnet coherence length $\xi_F = \hbar v_F/h_0$, where v_F is the Fermi velocity. In the clean limit, influence of misorientation of magnetizations on the Josephson current or conductance can not be attributed to the triplet correlations.^{19,20} Moreover, for noncollinear magnetizations, $\alpha \neq 0$ and π , both spin singlet and triplet pair amplitudes in ferromagnetic layers decay in the same oscillatory manner with distance from the FS interfaces.^{21,22}

In this paper, we study the Josephson effect and odd-frequency triplet superconductivity in clean and moderately disordered SFFS junctions where the magnetic interlayer consists of two monodomain ferromagnets having relative angle α between their in-plane magnetizations. Solving the Eilenberger equations we calculate singlet and triplet pair amplitudes, and the Josephson current. In contrast to the dirty limit case we find that for $0 < \alpha < \pi$, both spin singlet and triplet pair amplitudes in F layers are oscillating and power law decaying with distance from the FS interfaces. This decay gets faster as the impurity-scattering rate in ferromagnets is increased. The computed triplet amplitudes have opposite signs in the two magnet regions, penetrate into the

superconductors and monotonically decay over the superconducting coherence length, $\xi_S = \hbar v_F / \pi \Delta_0$, where Δ_0 is the superconducting pair potential, which is the same distance on which the singlet amplitude saturates to the bulk value. As in the previous work,¹⁹ no substantial impact of spin-triplet superconducting correlation on the Josephson current has been found. The critical value of the Josephson current I_c is a monotonic function of angle α when the junction is far enough from the $0 - \pi$ transitions. Otherwise, $I_c(\alpha)$ is a nonmonotonic function of α with characteristic dips related to the onset of $0 - \pi$ transitions, but this nonmonotonicity is a consequence of decreasing influence of the exchange potential with increasing misorientation of magnetizations.¹⁹ Influence of misorientation of magnetizations on the Josephson current can not be attributed to the appearance of triplet correlations: with increasing misorientation of magnetizations, $\alpha \rightarrow \pi$, the Josephson currents are the same as for parallel magnetizations, $\alpha = 0$, with correspondingly decreasing exchange potential, $h_0 \rightarrow 0$. Therefore, rotation of magnetizations in SFFS junctions is equivalent to the decreasing influence of the homogeneous exchange potential, in the absence of triplet correlations.

The paper is organized as follows. In Sec. II we present the model and the solutions of Eilenberger equations that we used to calculate the Josephson current and spin-singlet and -triplet pair amplitudes. In Sec. III we present the numerical results, and the conclusion in Sec. IV.

II. MODEL AND FORMALISM

We consider a clean SF₁F₂S heterojunction consisting of two superconductors (S), and two uniform monodomain ferromagnetic layers (F₁ and F₂) of thickness d_1 and d_2 , with misorientation angle α between their in-plane magnetizations (see Fig. 1). Interfaces between layers are fully transparent and magnetically inactive. Superconductors are described in the framework of quasiclassical theory of superconductivity, while the ferromagnetism is modeled by the Stoner model, using an exchange energy shift $2h_0$ between the spin subbands. Disorder is characterized by the mean free path $l = v_F \tau$, where τ is the average time between scattering on impurities and v_F is the Fermi velocity assumed to be the same everywhere. We consider the clean limit and moderately diffusive case when l is larger than the two characteristic lengths: the ferromagnetic exchange length $\xi_F = \hbar v_F / h_0$, and the superconducting coherence length $\xi_S = \hbar v_F / \pi \Delta_0$, where Δ_0 is the superconducting pair potential.

In this model the Eilenberger Green functions $g_{\sigma\sigma'}(x, v_x, \omega_n)$, $f_{\sigma\sigma'}(x, v_x, \omega_n)$, and $f_{\sigma\sigma'}^+(x, v_x, \omega_n)$ depend on the center-of-mass coordinate x along the junction axis x , on the angle θ of the quasiclassical trajectories with respect to x axis, $v_x = v_F \cos \theta$ being the projection of the Fermi velocity vector, and on the Mat-

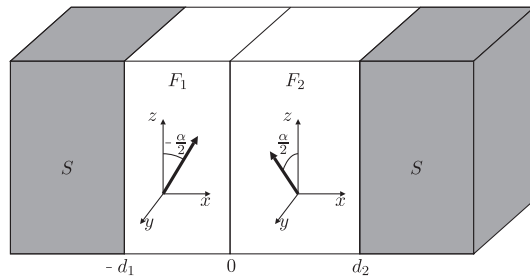


FIG. 1: Schematics of an SF₁F₂S heterojunction. The magnetization vectors lie in the y - z plane and form the opposite angles $\pm\alpha/2$ with respect to the z -axis.

subara frequencies $\omega_n = \pi k_B T (2n + 1)$, $n = 0, \pm 1, \pm 2$, etc. Spin indexes are $\sigma = \uparrow, \downarrow$.

The Eilenberger equation in spin \otimes particle-hole space can be written in the compact form

$$\hbar v_x \partial_x \check{g} + \left[\omega_n \hat{\tau}_3 \otimes \hat{1} - i \check{V} + \check{\Delta} + \hbar \langle \check{g} \rangle / 2\tau, \check{g} \right] = 0, \quad (2.1)$$

with normalization condition $\check{g}^2 = \hat{1}$. We indicate by $\check{\cdot}$ and $\check{\cdot}$ 2×2 and 4×4 matrices, respectively. The brackets $\langle \dots \rangle$ denote angular averaging over the Fermi surface (integration over θ) and $[\dots]$ denotes a commutator. Here, the quasiclassical Green functions

$$\check{g} = \begin{bmatrix} g_{\uparrow\uparrow} & g_{\uparrow\downarrow} & f_{\uparrow\uparrow} & f_{\uparrow\downarrow} \\ g_{\downarrow\uparrow} & g_{\downarrow\downarrow} & -f_{\downarrow\uparrow} & f_{\downarrow\downarrow} \\ f_{\uparrow\uparrow}^+ & f_{\uparrow\downarrow}^+ & -g_{\downarrow\downarrow} & -g_{\downarrow\uparrow} \\ -f_{\uparrow\uparrow}^+ & -f_{\uparrow\downarrow}^+ & -g_{\uparrow\downarrow} & -g_{\uparrow\uparrow} \end{bmatrix}, \quad (2.2)$$

are related to the corresponding Gor'kov-Nambu Green functions \check{G} integrated over the energy $\varepsilon_{\mathbf{k}} = \hbar^2 k^2 / 2m - \mu$,

$$\check{g} = \frac{i}{\pi} \int d\varepsilon_{\mathbf{k}} \check{G}. \quad (2.3)$$

The matrix \check{V} is given by

$$\check{V} = \hat{1} \otimes \text{Re} \left[\mathbf{h}(x) \cdot \hat{\boldsymbol{\sigma}} \right] + i \hat{\tau}_3 \otimes \text{Im} \left[\mathbf{h}(x) \cdot \hat{\boldsymbol{\sigma}} \right], \quad (2.4)$$

where components $\hat{\sigma}_x, \hat{\sigma}_y, \hat{\sigma}_z$ of the vector $\hat{\boldsymbol{\sigma}}$ and $\hat{\tau}_1, \hat{\tau}_2, \hat{\tau}_3$ are Pauli matrices in spin and particle-hole space, respectively. The in-plane, y - z , magnetizations of the neighboring F layers are not collinear in general, and the magnetic domain structure is described by the angle $\mp\alpha/2$ with respect to the z -axis, for the left (F₁) and right (F₂) ferromagnets, respectively. For simplicity, we assume equal magnitude of the exchange interaction in ferromagnetic domains, $\mathbf{h}(x) = h_0(0, \mp \sin \alpha/2, \cos \alpha/2)$, and $\Delta(x) = 0$ for $-d_1 < x < d_2$.

The matrix $\check{\Delta}$ is

$$\check{\Delta} = \begin{bmatrix} 0 & \hat{\tau}_1 \Delta \\ \hat{\tau}_1 \Delta^* & 0 \end{bmatrix}. \quad (2.5)$$

We assume that the superconductors are identical and, in the step-wise (non self-consistent) approximation, we take the pair potential Δ in the form

$$\Delta = \Delta_0 \left[e^{-i\phi/2} \Theta(-x - d_1) + e^{i\phi/2} \Theta(x - d_2) \right], \quad (2.6)$$

where Δ_0 is the bulk superconducting gap and ϕ is the macroscopic phase difference across the junction. The temperature dependence of Δ_0 is given by $\Delta_0(T) = \Delta_0(0) \tanh\left(1.74\sqrt{T_c/T - 1}\right)$.²⁵ Although the self-consistent calculations are needed when the proximity effect is strong between S and F layers,²¹ one would not expect this to qualitatively change the spatial variation of the Green functions.

In the clean limit, $\tau \rightarrow \infty$, solutions of Eq. (2.1) for the left superconductor ($x < -d_1$) can be written in the usual form for normal Green functions

$$g_{\uparrow\uparrow}(x) = \frac{\omega_n}{\Omega_n} + D_1 e^{\kappa_s x}, \quad (2.7)$$

$$g_{\uparrow\downarrow}(x) = D_2 e^{\kappa_s x}, \quad (2.8)$$

$$g_{\downarrow\uparrow}(x) = D_3 e^{\kappa_s x}, \quad (2.9)$$

$$g_{\downarrow\downarrow}(x) = \frac{\omega_n}{\Omega_n} + D_4 e^{\kappa_s x}, \quad (2.10)$$

and for anomalous Green functions

$$f_{\uparrow\uparrow}(x) = \frac{2\Delta}{2\omega_n + \hbar v_x \kappa_s} D_2 e^{\kappa_s x}, \quad (2.11)$$

$$f_{\uparrow\downarrow}(x) = \frac{\Delta}{\Omega_n} + \frac{2\Delta}{2\omega_n + \hbar v_x \kappa_s} D_1 e^{\kappa_s x}, \quad (2.12)$$

$$f_{\downarrow\uparrow}(x) = -\frac{\Delta}{\Omega_n} - \frac{2\Delta}{2\omega_n + \hbar v_x \kappa_s} D_4 e^{\kappa_s x}, \quad (2.13)$$

$$f_{\downarrow\downarrow}(x) = \frac{2\Delta}{2\omega_n + \hbar v_x \kappa_s} D_3 e^{\kappa_s x}, \quad (2.14)$$

with

$$\kappa_s = \frac{2\Omega_n}{\hbar v_F |\cos(\theta)|}, \quad (2.15)$$

and $\Omega_n = \sqrt{\omega_n^2 + |\Delta|^2}$. For the right superconductor ($x > d_2$), the solutions keep the same form with $\kappa_s \rightarrow -\kappa_s$ and new set of constants D'_1, \dots, D'_4 .

Solutions for the Green functions in the clean limit, $\tau \rightarrow \infty$, for the left ferromagnetic layer F₁, $-d_1 < x < 0$, can be written in the form

$$g_{\uparrow\uparrow}(x) = K_1 + i \tan(\alpha/4) K_2 e^{i\kappa_0 x} - i \tan(\alpha/4) K_3 e^{-i\kappa_0 x}, \quad (2.16)$$

$$g_{\uparrow\downarrow}(x) = K_2 e^{i\kappa_0 x} + \tan^2(\alpha/4) K_3 e^{-i\kappa_0 x} + \frac{i}{2} \tan(\alpha/2) [K_1 - K_4], \quad (2.17)$$

$$g_{\downarrow\uparrow}(x) = K_3 e^{-i\kappa_0 x} + \tan^2(\alpha/4) K_2 e^{i\kappa_0 x} - \frac{i}{2} \tan(\alpha/2) [K_1 - K_4], \quad (2.18)$$

$$g_{\downarrow\downarrow}(x) = K_4 - i \tan(\alpha/4) K_2 e^{i\kappa_0 x} + i \tan(\alpha/4) K_3 e^{-i\kappa_0 x}, \quad (2.19)$$

and

$$f_{\uparrow\uparrow}(x) = C_1 e^{-\kappa x} - i \tan(\alpha/4) C_2 e^{-\kappa - x} - i \tan(\alpha/4) C_3 e^{-\kappa + x}, \quad (2.20)$$

$$f_{\uparrow\downarrow}(x) = C_2 e^{-\kappa - x} - \tan^2(\alpha/4) C_3 e^{-\kappa + x} - \frac{i}{2} \tan(\alpha/2) [C_1 + C_4] e^{-\kappa x}, \quad (2.21)$$

$$f_{\downarrow\uparrow}(x) = -C_3 e^{-\kappa + x} + \tan^2(\alpha/4) C_2 e^{-\kappa - x} + \frac{i}{2} \tan(\alpha/2) [C_1 + C_4] e^{-\kappa x}, \quad (2.22)$$

$$f_{\downarrow\downarrow}(x) = C_4 e^{-\kappa x} - i \tan(\alpha/4) C_2 e^{-\kappa - x} - i \tan(\alpha/4) C_3 e^{-\kappa + x}, \quad (2.23)$$

where

$$\kappa_0 = 2h_0/\hbar v_x, \quad (2.24)$$

and

$$\kappa = 2\omega_n/\hbar v_x, \quad (2.25)$$

$$\kappa_- = 2(\omega_n - ih_0)/\hbar v_x, \quad (2.26)$$

$$\kappa_+ = 2(\omega_n + ih_0)/\hbar v_x. \quad (2.27)$$

The solution for the right ferromagnetic layer F₂, $0 < x < d_2$, can be obtained by substitution $\alpha \rightarrow -\alpha$, with

a new set of constants K'_1, \dots, K'_4 and C'_1, \dots, C'_4 . The complete solution requires one to determine 24 unknown coefficients: 4+4 in superconducting electrodes, and 8+8 in ferromagnetic layers. Boundary conditions of continuity of \check{g} at the three interfaces provide necessary 24 equations.

For $h_0 = 0$ solutions (2.16)-(2.19) reduce to the solutions for SNS junctions with $K_2 = K_3 = 0$ and $K_4 = K_1$. Solutions (2.20)-(2.23) reduce to the SNS case if we take $\alpha = 0$ and then $h_0 = 0$ with $C_1 = C_4 = 0$ and $C_3 = C_2$. Note that the same solutions are obtained for $\alpha = \pi$ and

$h_0 \neq 0$.

The supercurrent density is given by the normal Green function through the following expression

$$I(\phi) = \pi e N(0) k_B T \sum_{\omega_n} \sum_{\sigma} \langle v_x \text{Im} g_{\sigma\sigma}(v_x) \rangle, \quad (2.28)$$

where $N(0)$ is the density of states per spin at the Fermi level.

The zero-time pair amplitudes, singlet f_s , and triplet f_{t0} and f_{t1} , with 0 and ± 1 projections of the total spin of a pair, are defined in terms of anomalous Green functions as

$$f_s = \pi N(0) k_B T \sum_{\omega_n} (f_{\uparrow\downarrow} - f_{\downarrow\uparrow}), \quad (2.29)$$

$$f_{t0} = \pi N(0) k_B T \sum_{\omega_n} (f_{\uparrow\downarrow} + f_{\downarrow\uparrow}), \quad (2.30)$$

$$f_{t1} = \pi N(0) k_B T \sum_{\omega_n} (f_{\uparrow\uparrow} + f_{\downarrow\downarrow}). \quad (2.31)$$

The ground state in SFS junctions can be 0 or π state.²⁶ For $\phi = 0$ the singlet amplitude f_s is real, while the triplet amplitudes f_{t0} and f_{t1} are imaginary, and for $\phi = \pi$ the opposite is true. For $0 < \phi < \pi$, all the amplitudes are complex functions. In the figures, we will normalize all amplitudes to the value of f_s in bulk superconductors,

$$f_{sb} = \pi N(0) k_B T \sum_{\omega_n} \frac{\Delta_0}{\Omega_n}. \quad (2.32)$$

The influence of moderate disorder in ferromagnetic layers on the Josephson current and on the pair amplitudes is studied in the limit $h_0\tau/\hbar \gg 1$. From the term $\hbar\langle\dot{g}\rangle/2\tau$ in Eq. (2.1) we kept the largest contribution, which is $\langle g_{\sigma\sigma} \rangle$ calculated for $\tau \rightarrow \infty$. The contributions of $\langle f_{\sigma\sigma'} \rangle$ and $\langle g_{\sigma\bar{\sigma}} \rangle$ are neglected. Introducing $\langle g_{\uparrow\uparrow} \rangle = R + iI$, we find that $\langle g_{\downarrow\downarrow} \rangle = R - iI$. Numerical calculations show that R is independent of x , and $R \approx \text{sign}(\omega_n)$ for any α . The imaginary part I oscillates with x , except for $\alpha = 0$, but it is nontrivial only in the vicinity of $\omega_n = 0$. Therefore, the contribution of I to the pair amplitudes, as well as to the supercurrent, can be neglected, and the previous solutions Eqs.(2.16)–(2.23) are used by replacing only κ, κ_{\pm} , Eqs.(2.25)–(2.27), with

$$\tilde{\kappa} = \kappa + \frac{R}{\tau v_x}, \quad (2.33)$$

$$\tilde{\kappa}_- = \kappa_- + \frac{R}{\tau v_x}, \quad (2.34)$$

$$\tilde{\kappa}_+ = \kappa_+ + \frac{R}{\tau v_x}. \quad (2.35)$$

III. RESULTS

For simplicity, we consider a single transfer channel (one-dimensional case). We illustrate our results for symmetric junctions with relatively thin and thick ferromagnetic layers, $d_1 = d_2 = 50k_F^{-1}$ and $500k_F^{-1}$, and for low

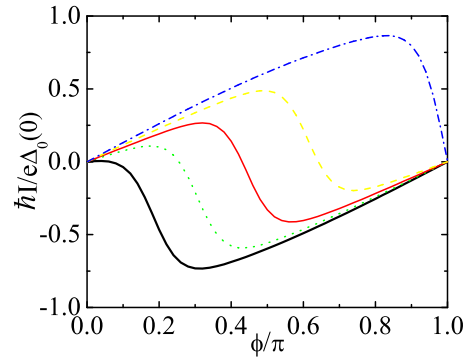


FIG. 2: (Color online) The current-phase relation $I(\phi)$ in the clean limit for $T/T_c = 0.1$, $h_0/E_F = 0.1$, $d_1 = d_2 = 50k_F^{-1}$, and five values of the misorientation angle: $\alpha = 0$ (thick solid curve), $\pi/3$ (dotted curve), $\pi/2$ (thin solid curve), $2\pi/3$ (dashed curve) and π (dash-dotted curve). The latter coincides with $I(\phi)$ in the corresponding SNS junction ($h_0 = 0$).

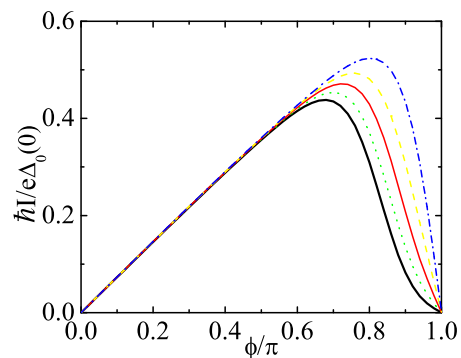


FIG. 3: (Color online) The current-phase relation $I(\phi)$ in the clean limit for $T/T_c = 0.1$, $h_0/E_F = 0.1$, $d_1 = d_2 = 500k_F^{-1}$, and five values of the misorientation angle: $\alpha = 0$ (thick solid curve), $\pi/3$ (dotted curve), $\pi/2$ (thin solid curve), $2\pi/3$ (dashed curve) and π (dash-dotted curve). The latter coincides with $I(\phi)$ in the corresponding SNS junction ($h_0 = 0$).

temperature $T/T_c = 0.1$. Superconductors are characterized with the zero temperature value of the bulk pair potential $\Delta_0(0)/E_F = 10^{-3}$, which corresponds to $\xi_S(0) = 636k_F^{-1}$. In order to achieve quantitatively reliable results within the quasiclassical approximation, we assume that all interfaces are fully transparent, the Fermi wave vectors in all metals are equal (k_F), and the ferromagnets are relatively weak, $h_0/E_F = 0.1$, which corresponds to $\xi_F = 20k_F^{-1}$.

Ballistic regime, $\tau \rightarrow \infty$, is illustrated in Figs. 2-5. The Josephson current is calculated from Eq. (2.28) for a single transverse channel (the angular averaging $\langle \dots \rangle$ reduces to one half of a discrete sum over $\theta = 0$ and

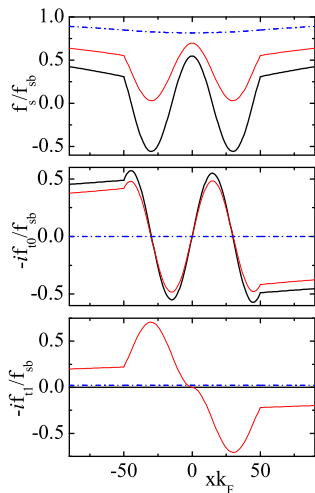


FIG. 4: (Color online) Spatial dependence of singlet and triplet pair amplitudes f_s , f_{t0} and f_{t1} , normalized to the bulk singlet pair amplitude f_{sb} , for $T/T_c = 0.1$, $h_0/E_F = 0.1$, $d_1 = d_2 = 50k_F^{-1}$, and three values of the misorientation angle: $\alpha = 0$ (thick solid curve), $\pi/2$ (thin solid curve) and π (dash-dotted curve). All amplitudes are calculated for $\phi = 0$ and $\theta = 0$.

$\theta = \pi$, and one-dimensional density of states per spin is $N(0) = 1/2\pi\hbar v_F$). We illustrate the current-phase relations $I(\phi)$ in Figs. 2 and 3 for five values of the angle between magnetizations in ferromagnetic layers, $\alpha = 0, \pi/3, \pi/2, 2\pi/3$, and π . Previous results obtained in Ref.¹⁹ by solving the Bogoliubov-de Gennes equation are exactly reproduced for this case of transparent interfaces and equal Fermi wave vectors. In particular, we see in Fig. 2 that the transition between 0 and π states can be induced by varying the misorientation angle α , including the coexistence of stable and metastable 0 and π states with dominant second harmonic.²⁷ However, non-monotonic dependence of the Josephson current $I(\phi)$ on α is due to decreasing influence of the exchange potential with increasing misorientation of magnetizations: $I(\phi)$ for noncollinear magnetizations ($\alpha \neq 0$) is practically equal to the one for homogeneous magnetization ($\alpha = 0$) with correspondingly smaller exchange energy. Influence of α on $I(\phi)$ can not be attributed directly to the appearance of odd triplet correlations. When the junction is far enough from the $0 - \pi$ transitions, the critical Josephson current is a monotonic function of α , Fig. 3. We emphasize that $I(\phi)$ curves for $\alpha = \pi$ are the same as in the corresponding SNS junctions ($h_0 = 0$) since the influence of opposite magnetizations in F layers of a symmetric SFFS junction cancels out in the clean limit and for transparent interfaces.

The spatial variation of the pair amplitudes is shown

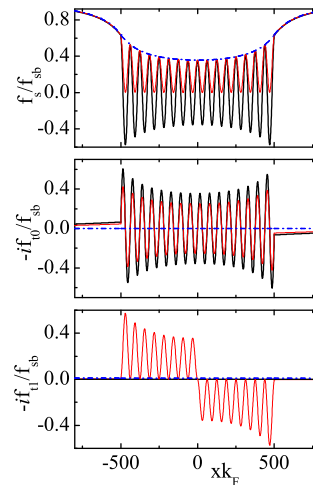


FIG. 5: (Color online) Spatial dependence of singlet and triplet pair amplitudes f_s , f_{t0} and f_{t1} , normalized to the bulk singlet pair amplitude f_{sb} , for $T/T_c = 0.1$, $h_0/E_F = 0.1$, $d_1 = d_2 = 500k_F^{-1}$, and three values of the misorientation angle: $\alpha = 0$ (thick solid curve), $\pi/2$ (thin solid curve) and π (dash-dotted curve).

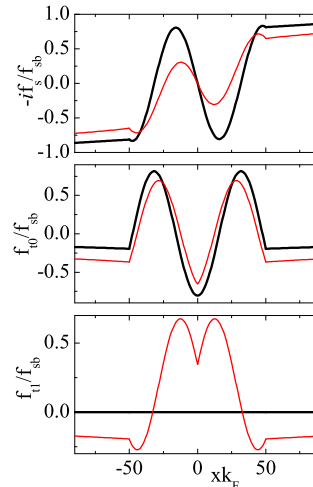


FIG. 6: (Color online) Spatial dependence of singlet and triplet pair amplitudes f_s , f_{t0} and f_{t1} , normalized to the bulk singlet pair amplitude f_{sb} , for $T/T_c = 0.1$, $h_0/E_F = 0.1$, $d_1 = d_2 = 50k_F^{-1}$, and two values of the misorientation angle: $\alpha = 0$ (thick solid curve) and $\pi/2$ (thin solid curve). All amplitudes are calculated for $\phi = \pi$ and $\theta = 0$.

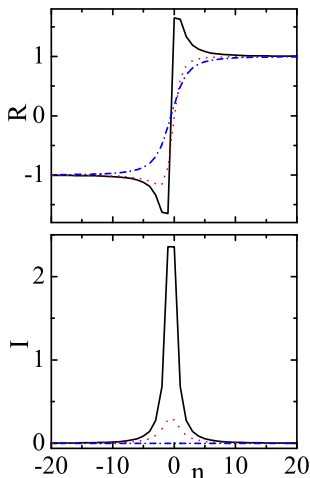


FIG. 7: (Color online) Real R and imaginary I parts of $\langle g_{\uparrow\uparrow} \rangle$ as functions of n in the Matsubara frequency $\omega_n = \pi k_B T (2n + 1)$ for $T/T_c = 0.1$, $h_0/E_F = 0.1$, $d_1 = d_2 = 50k_F^{-1}$, and three values of the misorientation angle: $\alpha = 0$ (solid curve), $\pi/2$ (dotted curve) and π (dash-dotted curve). The curves are calculated in the clean limit, $\tau \rightarrow \infty$, and for $\phi = 0$ and $\theta = 0$.

in Figs. 4 and 5 for thin and thick ferromagnetic layers, respectively, for $\theta = 0$ and for $\phi = 0$. Note that $f_s(\theta = \pi) = f_s(\theta = 0)$, and $f_{t1}(\theta = \pi) = f_{t1}(\theta = 0)$, while $f_{t0}(\theta = \pi) = -f_{t0}(\theta = 0)$. For $\phi = 0$ the singlet amplitude f_s is real, while the triplet amplitudes f_{t0} and f_{t1} are imaginary (Figs. 4 and 5), and for $\phi = \pi$ the opposite is true (Fig. 6). It can be seen that both spin singlet and triplet pair amplitudes decay in the same oscillatory manner with distance from the FS interfaces. Similar behavior of these correlations, i.e., the absence of monotonically decaying long-ranged triplet pair amplitude, which is in a striking contrast with the dirty-limit case,² explains the monotonic dependence of I_c on α far from the $0 - \pi$ transitions. For $\alpha = 0$, amplitudes f_s and f_{t0} oscillate with x around zero and $f_{t1} = 0$. For $\alpha = \pi/2$ the amplitude f_{t0} oscillates as a function of x as in the previous case, while f_s and f_{t1} oscillate in the same manner above or below zero. We find that f_{t0} and f_{t1} oscillate in phase and with the same characteristic length (proportional to $1/h_0$) as f_s , regardless of α , when $0 < \alpha < \pi$. Phase of f_s oscillations is shifted by π . We also find that triplet correlations penetrate into the superconductors and monotonically decay over ξ_S , the same characteristic length, on which the singlet amplitude saturates. For $\alpha = \pi$, when the magnetizations are antiparallel no triplet amplitudes exist and f_s monotonically decays away from the FS interfaces as in SNS junctions.

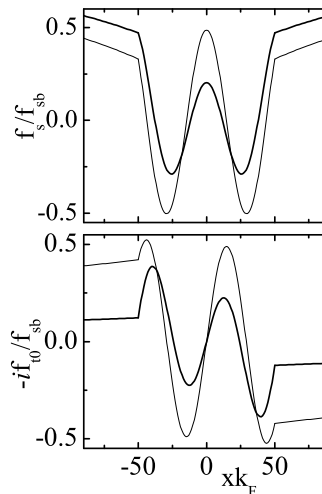


FIG. 8: Spatial dependence of singlet and triplet pair amplitudes f_s and f_{t0} , normalized to the bulk singlet pair amplitude f_{sb} , for parallel magnetizations, $\alpha = 0$, $T/T_c = 0.1$, $h_0/E_F = 0.1$, $d_1 = d_2 = 50k_F^{-1}$ and for two values of the impurity-scattering rate $\hbar/2\tau E_F = 0.001$ (thin solid curve) and 0.01 (thick solid curve).

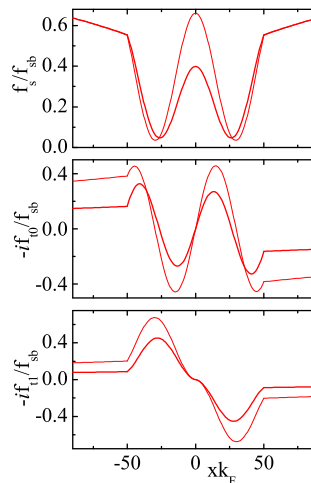


FIG. 9: (Color online) Spatial dependence of singlet and triplet pair amplitudes f_s , f_{t0} and f_{t1} , normalized to the bulk singlet pair amplitude f_{sb} , for orthogonal magnetizations, $\alpha = \pi/2$, $T/T_c = 0.1$, $h_0/E_F = 0.1$, $d_1 = d_2 = 50k_F^{-1}$ and for two values of the impurity-scattering rate $\hbar/2\tau E_F = 0.001$ (thin solid curve) and 0.01 (thick solid curve).

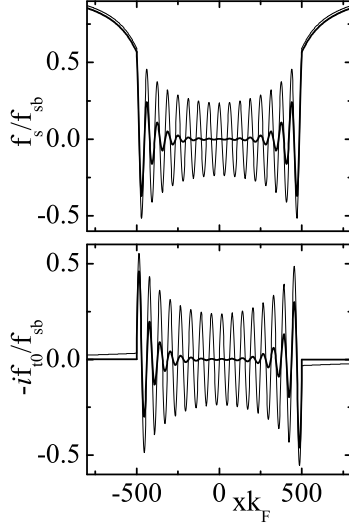


FIG. 10: Spatial dependence of singlet and triplet pair amplitudes f_s and f_{t0} , normalized to the bulk singlet pair amplitude f_{sb} , for parallel magnetizations, $\alpha = 0$, $T/T_c = 0.1$, $h_0/E_F = 0.1$, $d_1 = d_2 = 500k_F^{-1}$ and for two values of the impurity-scattering rate $\hbar/2\tau E_F = 0.001$ (thin solid curve) and 0.01 (thick solid curve).

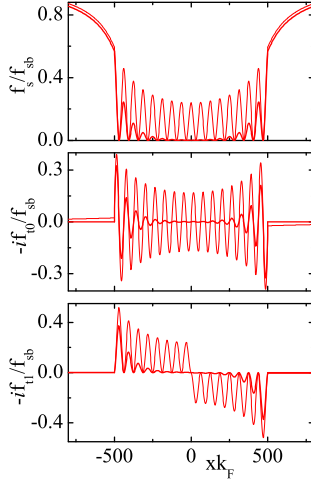


FIG. 11: (Color online) Spatial dependence of singlet and triplet pair amplitudes f_s , f_{t0} and f_{t1} , normalized to the bulk singlet pair amplitude f_{sb} , for orthogonal magnetizations, $\alpha = \pi/2$, $T/T_c = 0.1$, $h_0/E_F = 0.1$, $d_1 = d_2 = 500k_F^{-1}$ and for two values of the impurity-scattering rate $\hbar/2\tau E_F = 0.001$ (thin solid curve) and 0.01 (thick solid curve).

In order to study the effect of finite τ , we have calculated $\langle g_{\sigma\sigma} \rangle$ in the clean limit ($\tau \rightarrow \infty$) as the largest contribution to the term $\hbar\langle \check{g} \rangle / 2\tau$ in Eq. (2.1). In Fig. 7 the typical dependence of real and imaginary parts of $\langle g_{\sigma\sigma} \rangle$ on the Matsubara frequencies is illustrated for thin ferromagnetic layers and three values of $\alpha = 0, \pi/2, \pi$. Taking $R \approx \text{sign}(\omega_n)$ for any α , and neglecting contribution of I which is nontrivial only in the vicinity of $\omega_n = 0$, we calculate \check{g} from the clean limit solutions, Eqs. (2.16)–(2.23), replacing only κ, κ_{\pm} with $\tilde{\kappa}, \tilde{\kappa}_{\pm}$, given by Eqs. (2.33)–(2.35).

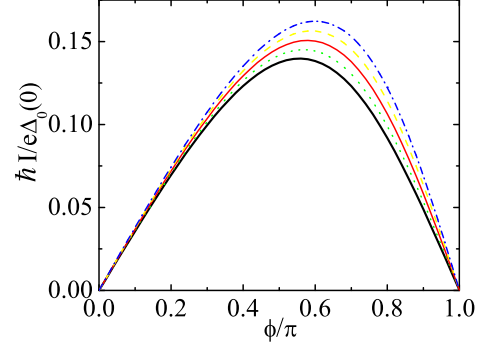


FIG. 12: (Color online) The current-phase relation $I(\phi)$ for weakly disordered ferromagnets $\hbar/2\tau E_F = 0.001$, for $T/T_c = 0.1$, $h_0/E_F = 0.1$, $d_1 = d_2 = 500k_F^{-1}$, and five values of the misorientation angle: $\alpha = 0$ (thick solid curve), $\pi/3$ (dotted curve), $\pi/2$ (thin solid curve), $2\pi/3$ (dashed curve) and π (dash-dotted curve).

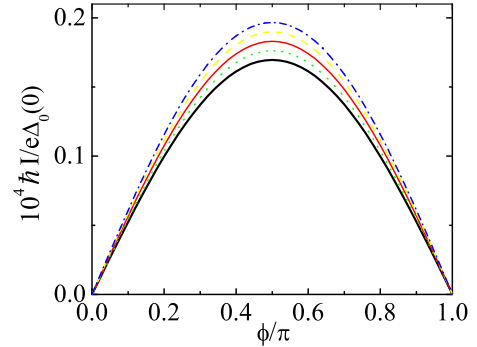


FIG. 13: (Color online) The current-phase relation $I(\phi)$ for weakly disordered ferromagnets $\hbar/2\tau E_F = 0.01$, for $T/T_c = 0.1$, $h_0/E_F = 0.1$, $d_1 = d_2 = 500k_F^{-1}$, and five values of the misorientation angle: $\alpha = 0$ (thick solid curve), $\pi/3$ (dotted curve), $\pi/2$ (thin solid curve), $2\pi/3$ (dashed curve) and π (dash-dotted curve).

The influence of moderate disorder in ferromagnets on the pair amplitudes is illustrated in Figs. 8-11 for the parallel ($\alpha = 0$) and the orthogonal ($\alpha = \pi/2$)

magnetizations, for two values of the scattering rates, $\hbar/2\tau E_F = 0.001$ and 0.01 . It can be seen that the only difference from the $\tau \rightarrow \infty$ case is the faster decay with the distance from FS interfaces. However, all amplitudes, singlet and triplet, decay with the same characteristic length. We can not see that the triplets are longer-ranged than the singlets. The influence of scattering on impurities in ferromagnets on the Josephson current is shown in Fig. 12, for thick ferromagnetic layers and for $\hbar/2\tau E_F = 0.001$. Comparison with Fig. 3 shows that current-phase relation is almost sinusoidal and the critical current is three times smaller. For ten times larger scattering rate, $\hbar/2\tau E_F = 0.01$, numerical calculation gives exactly sinusoidal $I(\phi)$ and four order of magnitudes smaller critical current, Fig. 13.

IV. CONCLUSION

We have studied the Josephson effect in clean and moderately disordered SFFS junctions containing conventional (*s*-wave) superconductors, two mono-domain ferromagnetic layers with arbitrary angle α between in-plane magnetizations, and fully transparent interfaces. We have calculated the Josephson current and both singlet and odd in frequency triplet amplitudes in the clean limit and for moderate disorder in ferromagnets by solving the Eilenberger quasiclassical equations analytically in the step-wise (non self-consistent) approximation for the pair potential. Using quasiclassical approach we limited our considerations to the case of equal Fermi wave vectors, relatively weak ferromagnets and transparent interfaces. For the Josephson current we reproduced previous results for the clean limit¹⁹ and have found crossover

to the dirty limit case for finite impurity-scattering rate which leads to sinusoidal current-phase relation and considerably smaller value of the critical current. In particular, transitions between 0 and π states are induced by varying the relative orientation of magnetizations, both in clean and diffusive junctions.^{19,28,29} However, in the clean limit this is simply the effect of decreasing influence of the exchange potential with increasing misorientation of magnetizations and far from 0 – π transitions the critical Josephson current monotonically depends on the angle between magnetizations. This can be seen in the calculated spatial variation of the pair amplitudes. We find that for $0 < \alpha < \pi$, both spin singlet and triplet pair amplitudes in F layers decay in the same oscillatory manner with distance from the FS interfaces. This decay gets faster as the impurity-scattering rate in ferromagnets is increased, but characteristic length of oscillations is unchanged. The computed triplet amplitude f_{t1} has opposite signs in the two magnet regions, penetrates into the superconductors and monotonically decays over the same distance, which is the superconducting coherence length, as the singlet amplitude f_s saturates to the bulk value. In contrast to the dirty limit case,³ no substantial impact of odd in frequency spin-triplet superconducting correlations on the Josephson current has been found in the ballistic and moderately diffusive regimes.

V. ACKNOWLEDGMENT

ZR thanks Gerd Schön, Yasuhiro Asano, and Ivan Božović for useful discussions. The work was supported by the Serbian Ministry of Science, Project No. 141014.

-
- ¹ F. S. Bergeret, A. F. Volkov, and K. B. Efetov, Phys. Rev. Lett. **86**, 3140 (2001).
² A. F. Volkov, F. S. Bergeret, and K. B. Efetov, Phys. Rev. Lett. **90**, 117006 (2003).
³ F. S. Bergeret, A. F. Volkov, and K. B. Efetov, Rev. Mod. Phys. **77**, 1321 (2005).
⁴ R. S. Keizer, S. T. B. Goennenwein, T. M. Klapwijk, G. Miao, G. Xiao, and A. Gupta, Nature **439**, 825 (2006).
⁵ M. Eschrig and T. Löfwander, Nature Phys. **4**, 138 (2008).
⁶ Y. Asano, Y. Tanaka, and A. Golubov, Phys. Rev. Lett. **98**, 107002 (2007).
⁷ V. L. Berezinskii, Pis'ma Zh. Eksp. Teor. Fiz. **20**, 628 (1974) [JETP Lett. **20**, 287 (1974)].
⁸ D. Solenov, I. Martin, and D. Mozyrsky, Phys. Rev. B **79**, 132502 (2009).
⁹ Ya. V. Fominov, A. A. Golubov, and M. Yu. Kupriyanov, JETP Lett. **77**, 510 (2003).
¹⁰ C. Y. You, Ya. B. Bazaliy, J. Y. Gu, S. J. Oh, L. M. Litvak, and S. D. Bader, Phys. Rev. B **70**, 014505 (2004).
¹¹ T. Löfwander, T. Champel, J. Durst, and M. Eschrig, Phys. Rev. Lett. **95**, 187003 (2005).
¹² Yu. S. Barash, I. V. Bobkova, and T. Kopp, Phys. Rev. B **66**, 140503(R) (2002).
¹³ I. B. Sperstad, J. Linder, and A. Sudbø, Phys. Rev. B **78**, 104509 (2008).
¹⁴ M. Eschrig, J. Kopu, J. C. Cuevas, and G. Schön, Phys. Rev. Lett. **90**, 137003 (2003).
¹⁵ Ya. M. Blanter and F. W. J. Hekking, Phys. Rev. B **69**, 024525 (2004).
¹⁶ J. Linder, M. Zareyan, and A. Sudbø, Phys. Rev. B **79**, 064514 (2009).
¹⁷ K. L. Usadel, Phys. Rev. Lett. **25**, 507 (1970).
¹⁸ G. Eilenberger, Z. Phys. **214**, 196 (1968).
¹⁹ Z. Pajović, M. Božović, Z. Radović, J. Cayssol, and A. I. Buzdin, Phys. Rev. B **74**, 184509 (2006).
²⁰ M. Božović and Z. Radović, New J. Phys. **9**, 264 (2007).
²¹ K. Halterman, P. H. Barsic, and O. T. Valls, Phys. Rev. Lett. **99**, 127002 (2007).
²² K. Halterman, O. T. Valls, and P. H. Barsic, Phys. Rev. B **77**, 174511 (2008).
²³ Z. Radović, N. Lazarides, and N. Flytzanis, Phys. Rev. B **68**, 014501 (2003).
²⁴ F. Konschelle, J. Cayssol, and A. I. Buzdin, Phys. Rev. B **78**, 134505 (2008).

- ²⁵ B. Muhlschlegel, *Z. Phys.* **155**, 313 (1959).
- ²⁶ A. I. Buzdin, *Rev. Mod. Phys.* **77**, 935 (2005).
- ²⁷ Z. Radović, L. Dobrosavljević-Grujić, and B. Vujčić, *Phys. Rev. B* **63**, 214512 (2001).
- ²⁸ A. A. Golubov, M. Yu. Kupriyanov, and Ya. V. Fominov, *JETP Lett.* **75**, 190 (2002).
- ²⁹ F. S. Bergeret, A. F. Volkov, and K. B. Efetov, *Phys. Rev. B* **68**, 064513 (2003).